Prediction of the Vapor−Liquid Interfacial Tension of Nonassociating and Associating Fluids with the SAFT-VR Density Functional Theory†

ARTICLE *in* THE JOURNAL OF PHYSICAL CHEMISTRY C · SEPTEMBER 2007

Impact Factor: 4.77 · DOI: 10.1021/jp072344i

5 AUTHORS, INCLUDING:

Felipe J. Blas
Universidad de Huelva
75 PUBLICATIONS **1,823** CITATIONS

SEE PROFILE

Prediction of the Vapor−Liquid Interfacial Tension of Nonassociating and Associating Fluids with the SAFT-VR Density Functional Theory†

Guy J. Gloor,‡ George Jackson,*,‡ F. J. Blas,§ E. Martín del Río,⊥ and E. de Miguel§

Department of Chemical Engineering, Imperial College London, South Kensington Campus, London SW7 2BY, UK; Departamento de Física Aplicada, Facultad de Ciencias Experimentales, Universidad de Huelva, 21071, Huelva, Spain; Departamento de Ingeniería Eléctrica y Térmica, Escuela Politécnica Superior de La Rábida, Universidad de Huelva, 21819 Huelva, Spain

Received: March 24, 2007; In Final Form: June 26, 2007

The SAFT-VR DFT Helmholtz free energy density functional [Gloor, G. J.; Jackson, G.; Blas, F. J.; Martín del Río, E.; de Miguel, E. *J. Chem. Phys.* **2004**, *121*, 12740] is used to describe the vapor−liquid interface of nonassociating and associating molecules ranging in size from small molecules to long chains. The functional, which is based on the statistical associating fluid theory for attractive potentials of variable range (SAFT-VR) description of the homogeneous fluid [Gil-Villegas, A.; Galindo, A.; Whitehead, P. J.; Mills, S. J.; Jackson, G.; Burgess, A. N. *J. Chem. Phys*. **1997**, *106*, 4168], is constructed by partitioning the free energy density into a reference term (which incorporates all of the short-range interactions and is treated locally) and an attractive perturbation (which incorporates the long-range dispersion interactions). This functional accounts explicitly for the correlations between the segments using a density-averaged correlation function incorporated into the perturbative term in a similar way to that proposed by Toxvaerd. The SAFT-VR DFT formalism is used to examine the vapor−liquid interfacial tension of a number of pure components, including: *n*-alkanes; small associating molecules, such as water; linear alkan-1-ols; and some selected replacement refrigerants. In the case of the hydrocarbons and other weakly polar substances, the surface tension can be predicted from intermolecular parameters derived in the usual way from the bulk fluid phase equilibria (vapor-pressure and saturated liquid density). By contrast, when one describes the interfacial properties of associating compounds, it is important to include the surface tension data as well as the bulk vapor−liquid phase equilibria in developing the intermolecular potential model. This provides a means of determining the balance between the dispersive and associative (hydrogen bonding) contributions to the intermolecular potential. The use of interfacial data in the refinement of the potential model allows one to obtain a reliable set of parameters, which can be used to predict the bulk and interfacial properties of mixtures for a broad range of thermodynamic conditions.

1. Introduction

Interfacial properties of complex fluids are of fundamental importance in broad areas of applied science and engineering. In addition to the inherent interest in the fundamental nature of interfaces, a detailed understanding of the thermodynamics of interfaces is essential from a practical perspective. A knowledge of the interfacial tension, interfacial profiles, interfacial thickness, and relative Gibbs adsorption of a given component, among other properties, are the key to the efficient and optimal design of separation processes, catalysts, and the complex formulations that are common in the petrochemical, detergent, paint, nutrition, hygiene, personal care, pharmaceutical, and biomedical sectors.

Large strides have been made in understanding and developing theories for inhomogeneous systems since the early days of Laplace and Young (mechanical view) and van der Waals (local thermodynamic square-gradient approach),[1−3] but an accurate prediction of the interfacial properties of complex systems is still very much in its infancy. This is in contrast with our current ability to describe the bulk thermodynamic properties and phase equilibria of fluids and fluid mixtures of comparative complexity with a host of analytical theories. In particular, standard perturbative and integral equation approaches can be employed to predict the bulk behavior of fluid mixtures as complex as aqueous solutions, amphiphiles, polymers, and electrolytes.[4] One of the most successful modern equations of state for complex fluids is the statistical associating fluid theory (SAFT) developed by Gubbins and co-workers[5,6] which is based on Wertheim's[7−12] first-order thermodynamic perturbation theory (TPT1) for associating systems. For a more recent description of the TPT1 formalism, the reader is directed to references 13 and 14. The SAFT approach (in its many incarnations) is seen to very accurately describe the fluid phase behavior of a wide range of systems, from small strongly associating molecules to long-chain molecules and charged systems (see the comprehensive reviews of Müller and Gubbins[15,16] for further details).

Following the first molecular description of van der Waals,[1,2,17] a great deal of effort has been expended in developing a reliable theoretical platform for the interfacial properties of inhomogeneous systems. The parachor method introduced by Macleod[18,19] is usually employed to correlate the interfacial tension with the

† Part of the "Keith E. Gubbins Festschrift".

* Corresponding author. E-mail: g.jackson@imperial.ac.uk.
‡ Imperial College London.
§ Departamento de Física Aplicada, Universidad de Huelva.
⊥ Departamento de Ingeniería Eléctrica y Térmica, Universidad de Huelva.

10.1021/jp072344i CCC: $37.00
Published on Web 09/06/2007 PAGE EST: 9.3

difference in densities of the coexisting fluid phases. Though it was developed as an empirical approach, the Macleod parachor was placed on a firm statistical mechanical footing by Fowler,[20] who showed it can be derived in the case of a stepwise density profile as an explicit function of the intermolecular potential. In conjunction with the corresponding-states principle of Guggenheim,[21,22] the Macleod parachor is the most widely used empirical method for the interfacial tension. The corresponding-states approaches provide a very accurate description of the interfacial properties of a variety of systems, but their predictive capability depends on the reference fluid that is chosen and the empirical relationships that are used. The square-gradient theory (SGT), which is rooted in the early treatment of van der Waals[1,2] and was rediscovered by Cahn and Hilliard,[23] and its many versions and extensions (e.g., see references 24−26) provide a more formal route to the interfacial density profile and tension of fluid systems. The SGT is normally expressed in terms of a local free-energy density (obtained from an equation of state) and the second-order derivative of the density profile with respect to the spatial coordinates. In recent years the square-gradient method has been combined with the SAFT free energy to determine the interfacial properties of a number of pure fluids and mixtures.[27−34] Though the SAFT−SGT approach has been shown to provide a good representation of the surface tension, the need for empirical adjustable parameters, the so-called "influence" parameters, limits the predictive capabilities of the method particularly in the case of mixtures.

The most successful of the modern approaches are invariably based on a detailed molecular density functional theory (DFT). The classical DFT methods owe much to the SGT formalism of van der Waals, which can be regarded as the first variational treatment for inhomogeneous fluids. In a DFT description, the free energy of the system is expressed as a functional of the spatially varying single-particle density. The approach has been described in detail by a number of authors, including Evans,[17] Davis,[35] Winkelmann,[36] and Wu,[37] who have discussed the general formalism and the various approximations that are commonly employed, including perturbation expansions, the local density approximation (LDA), and the weighted density approximation (WDA). Various forms of the SAFT description for homogeneous fluids have now been used to construct free-energy functionals for use in a classical DFT treatment of inhomogeneous fluids and confined systems.[38−46] For a more comprehensive review of the broader use of the Wertheim treatment of associating fluids (which is at the core of the SAFT approaches) in DFT the reader is directed to our previous papers[38,41] and references therein.

The goal of this work is to predict the vapor−liquid interfacial properties of a number of complex fluids using the Helmholtz free energy functional that we recently proposed for associating chain molecules.[41] The functional is based on the statistical associating fluid theory for attractive potentials of variable range (SAFT-VR) of the bulk fluid.[47] The free energy density is partitioned into a reference term, which incorporates all of the short-range interactions (the repulsive hard-sphere, the chain, and the association contributions) and is treated locally (LDA), and an attractive perturbation, which incorporates the long-range dispersion interactions. An adequate treatment of the correlations in the attractive term is crucial for an accurate description of both the bulk fluid phase equilibria and the interfacial properties. The correlations are included in the DFT using an average bulk pair distribution function in a way that is similar to the approach employed by Toxvaerd.[48] An accurate theory for the vapor−liquid interfacial profiles and surface tension of associating molecules with dispersion interactions of variable range is obtained in this way.

We apply this theory to predict the vapor−liquid interfacial properties for a comprehensive selection of representative pure substances, including nonpolar chain molecules (*n*-alkanes), small associating molecules (water), associating chain molecules, (*n*-alkan-1-ols), and some polar molecules (replacement hydrofluorocarbon refrigerants). For nonassociating (nonpolar) substances, intermolecular potential parameters obtained by refining to the experimental vapor−liquid phase envelope and vapor pressure allow for an accurate prediction of the interfacial properties. For substances with strong associating (and polar) interactions, the parameters obtained from a description of the experimental vapor−liquid phase equilibria alone do not usually provide an adequate prediction of the interfacial properties. For these complex associating fluids, a number of molecular models characterized by distinctly different sets of parameters are seen to describe the vapor−liquid phase envelope with essentially equivalent quality.[40,49] In this work, we show that a simultaneous assessment of the vapor−liquid phase equilibria and surface tension data can help one to obtain a unique set of "optimal" molecular parameters for associating substances. With such a procedure, the theory provides an accurate representation of both the vapor−liquid phase envelope and the interfacial properties. This work is seen as the first step in developing a general treatment for describing the interfacial properties of mixtures of associating chainlike molecules.

The rest of the paper is organized as follows: in Section 2, we present the most relevant features of the molecular model and theory, the results and discussion are presented in Section 3, and the conclusions are given in Section 4.

2. Molecular Model and Theory

The molecular model and theory that is used to determine the bulk phase behavior and the interfacial properties of nonassociating and associating chain molecules are briefly described before the results for the vapor−liquid phase equilibria and surface tension are presented.

As in earlier work,[38−41] the molecules are modeled following a simple unit-atom approach, in which m hard spherical attractive segments of diameter σ are bonded to form chains, and hydrogen-bonding sites are incorporated to mediate the association interactions where necessary. In the particular case of linear *n*-alkanes and *n*-alkan-1-ols, this model takes into account the main attributes of the molecular architecture of the chain, including the segment connectivity (to represent topological constraints and internal flexibility), excluded volume effects, and attractive interactions between the different segments that form the molecules (inter- and intramolecular dispersion interactions are treated). It is to be noted that some of the finer details of the chain conformation, such as branching, are incorporated only in an indirect approximate manner.

Pairwise repulsive, dispersive (van der Waals), and associative (hydrogen bonding) interactions are considered. In our particular model, the repulsive and dispersive interactions between two spherical segments making up the chain are described by a simple square-well potential,

$$\phi(r) = \begin{cases} \infty & r \le \sigma \\ -\epsilon & \sigma < r \le \lambda\sigma \\ 0 & r > \lambda\sigma \end{cases} \quad (1)$$

where r denotes the distance between the centers of the two segments, and $\lambda\sigma$ denotes the range of the dispersive interaction of depth ϵ. In the SAFT-VR approach, the variable range of

the attractive interactions plays an important role in describing the dispersion interactions of molecules with varying degrees of polarity.[47] A number, *m*, of these square-well segments are bonded together to form the chain. The association contribution is modeled by considering additional off-center sites (placed a distance r_d from the center of a given segment) which interact through a square-well potential of shorter range r_c. The interaction of a site A on one segment with a site B on another is given by

$$\phi_{AB}(r_{AB}) = \begin{cases} -\epsilon_{AB} & r_{AB} < r_c \\ 0 & r_{AB} > r_c \end{cases} \quad (2)$$

where r_{AB} is the distance between the centers of the two associating sites. Despite its simplicity, our molecular model includes the relevant features of the physics of the interaction between associating chain molecules.

The interfacial properties of selected molecules are studied within the context of a DFT based on the SAFT-VR free energy. In what follows, we give a brief account of the theory; further details can be found in reference.[41] A standard perturbative approach[17,36] is employed in which the intermolecular potential is separated into a reference term and a perturbation term. The former includes the (repulsive) hard-sphere interaction between molecular segments and the repulsive contribution due to the formation of a molecular chain as well as those interactions arising from the association contribution; the perturbation term includes the contribution due to the attractive square-well interactions between the monomeric segments.

For an open system in a volume *V*, at a temperature *T*, and a chemical potential μ (and in the absence of external fields), the grand potential functional $\Omega[\rho(r)]$ is given by[17]

$$\Omega[\rho(r)] = A[\rho(r)] - \mu \int \mathrm{d}r\, \rho(r) \quad (3)$$

where $A[\rho(r)]$ is the intrinsic Helmholtz free energy functional, and $\rho(r)$ is the density profile. The minimal value of $\Omega[\rho(r)]$ is the equilibrium grand potential of the system, and the corresponding equilibrium density profile $\rho_{eq}(r)$ satisfies the following condition:[17]

$$\left.\frac{\delta\Omega[\rho(r)]}{\delta\rho(r)}\right|_{eq} = \left.\frac{\delta A[\rho(r)]}{\delta\rho(r)}\right|_{eq} - \mu = 0 \quad (4)$$

The perturbative scheme leads to a natural partitioning of the free energy into reference (ref) and perturbative attractive (att) terms:

$$A[\rho(r)] = A^{ref}[\rho(r)] + A^{att}[\rho(r)] \quad (5)$$

The reference term is taken to incorporate all of the contributions to the free energy due to short-range interactions and can be expressed as

$$A^{ref}[\rho(r)] = A^{ideal}[\rho(r)] + A^{hs}[\rho(r)] + A^{chain}[\rho(r)] + A^{assoc}[\rho(r)] + A_2[\rho(r)] \quad (6)$$

Here, A^{ideal} is the usual ideal-gas contribution. The term A^{hs} is the (residual) contribution for an inhomogeneous system of hard spheres resulting form the repulsive interactions between monomers. This contribution is treated within a LDA, which implies that the hard-sphere contribution to the free energy of the inhomogeneous system is approximated by that of an equivalent homogeneous system of hard spheres evaluated at the local density $\rho(r)$. This approximation fails for highly oscillatory density profiles (such as those found at a solid surface) but provides a good description of the vapor−liquid interface. We make use of the Carnahan and Starling[14,50] expression for the residual free energy of the homogeneous hard-sphere system. The term A^{chain} in eq 6 denotes the contribution to the free energy due to the formation of chains of *m* square-well segments. This contribution follows as a limit of the standard Wertheim first-order thermodynamic perturbation theory (TPT1) of association.[12] Similarly, A^{assoc} represents the contribution due to association and is described within the Wertheim TPT1 approach.[11,12] In the present formulation, both the chain and associative contributions are incorporated into the free-energy functional at the LDA level because the interactions they represent are short range in nature. The last contribution, A_2 in eq 6, corresponds to the second-order term in a Barker and Henderson[51] high-temperature perturbation expansion of the free energy, which is described with the local compressibility approximation (LCA). In the LCA, one assumes that the second-order fluctuation of the attractive energy can be related directly to the compressibility of a hard-sphere reference fluid, a short-range repulsive contribution that can be treated locally within a DFT approach. Though strictly, one should include this attractive contribution in the perturbative term of the DFT, such an approximation allows one to recover the SAFT-VR free energy of the homogeneous bulk phases.

The first-order perturbative term A^{att} in eq 5 includes the contributions resulting from the attractive square-well interactions between the monomeric segments. In our approach, this is given by[17,35,36]

$$A^{att}[\rho(r)] = \frac{1}{2}\int \mathrm{d}r\, m\rho(r) \int \mathrm{d}r'\, m\rho(r')\, g^{ref}(r, r'; \rho(r), \rho(r'))\, \phi^{att}(|r - r'|) \quad (7)$$

where g^{ref} denotes the pair distribution function of the reference system (here described by that of a system of hard spheres), and ϕ^{att} is the attractive part of the segment−segment square-well potential. Because little is known of the pair distribution function of the inhomogeneous hard-sphere fluid, we assume that this function can be approximated by the pair distribution function of a homogeneous system of hard spheres evaluated at a mean density defined as $\bar{\rho} = (\rho(r) + \rho(r'))/2$. In a manner consistent with the SAFT-VR treatment of the bulk fluid,[47] the pair distribution function can be further approximated by its value at contact for an equivalent system with an effective density $\bar{\rho}_{eff}$ (which is a function of the mean density $\bar{\rho}$ and the range λ of the potential[41,47]). The final expression for the perturbative dispersive term used in the SAFT-VR DFT approach is given by

$$A^{att}[\rho(r)] = \frac{1}{2}\int \mathrm{d}r\, m\, \rho(r) \int \mathrm{d}r'\, m\rho(r') g^{hs}(\sigma;\bar{\rho}_{eff}) \phi^{att}(|r - r'|) \quad (8)$$

Within this approach, the free energy given by eq 5 reduces to the bulk SAFT-VR expression for homogeneous systems[47] when $\rho(r)$ is the bulk average number density ρ.

The equilibrium density profile follows from the solution of the Euler−Lagrange relation, eq 4. In this study, we consider planar vapor−liquid interfaces which are assumed to be perpendicular to the *z* axis, and thus, $\rho(r) \equiv \rho(z)$, where *z* is the distance normal to the interface. As in our previous paper,[41] a numerical integration of eq 4 is performed by starting from a trial density profile ρ_{old} with limiting densities that correspond

to the vapor and liquid equilibrium bulk densities (obtained as described in reference 47). This results in a new density profile ρ_{new}, and the process is repeated using a standard iterative scheme until the full density profile changes by no more than a specified tolerance.[52]

Once the equilibrium density profile $\rho_{eq}(z)$ is known, the surface tension can be determined from the simple thermodynamic relation

$$\gamma = \frac{\Omega + PV}{\mathcal{A}} \tag{9}$$

where $\mathcal{A}$ is the interfacial area and P is the bulk pressure.

3. Results and Discussion

In this work, we apply the SAFT-VR DFT to predict the phase equilibria and interfacial properties of representative nonassociating and associating substances, focusing on the surface tension of the vapor−liquid interface.

As with other equations of state, a number of molecular parameters are required in the SAFT-VR DFT formalism to describe the bulk thermodynamic and interfacial properties of real substances. Typically, these molecular parameters are determined by an optimization procedure in which the predicted and experimental vapor pressure, saturated liquid density and, in some cases, saturated vapor density are used to construct a least-square objective function.[52] The near critical data ($T > 0.9T_c$, with T_c being the critical temperature) is not usually considered because the description of the critical point with a classical equation of state is not appropriate; a more rigorous description requires the use of a renormalization group or extended scaling approach that is beyond the scope of our work. Once a refined set of intermolecular potential parameters are determined (corresponding to an "optimal" description of the fluid phase equilibria), the density profiles and surface tension are calculated for a range of temperature along the saturation line using the numerical procedure described in references.[40,41]

The SAFT equation of state is used routinely to describe the fluid phase equilibria of pure substances and mixtures of associating and nonassociating substances. Though the solution of the associative contribution to the free energy can be demanding, especially in the case of mixtures, the treatment of associating fluids in themselves does not pose a particular problem. The main complication with associating systems arises in the parameter optimization procedure, which results in a certain degree of degeneracy in the sets of molecular parameters that are obtained.[40,49] We recall that four parameters are required to fully specify the thermodynamics of nonassociating systems within the SAFT-VR approach, while at least two additional parameters are needed for associating molecules (depending on the associative scheme that is employed). For the associating systems, the objective function can turn out to be nonconvex (with numerous local minima of similar value) so that models characterized by different sets of parameters will represent the experimental data with an apparently equivalent quality.

Part of the difficulty in estimating the SAFT parameters for associating compounds is that though the vapor−liquid equilibria is governed by the magnitude of the total cohesive energy (i.e., attractive and associative), the bulk-phase separation does not appear to be very sensitive to the precise partitioning of the attractive and associative contributions. In this work we make use of interfacial experimental data to help in the refinement of the molecular parameters of associating substances. As will become clear in the following sections, the vapor−liquid interfacial tension is more sensitive to the precise partitioning of the energetic contributions.

TABLE 1: SAFT-VR Square-Well Intermolecular Potential Parameters for *n*-Alkanes Optimized to the Vapor−Liquid Equilibria Alone[61a]

substance	m	λ	σ/Å	(ϵ/k)/K
CH_4	1.000	1.448	3.685	167.3
C_2H_6	1.333	1.423	3.811	249.2
C_3H_8	1.667	1.454	3.890	260.9
C_4H_{10}	2.000	1.492	3.933	259.6
C_5H_{12}	2.333	1.506	3.943	264.6
C_6H_{14}	2.667	1.549	3.940	251.7
C_7H_{16}	3.000	1.557	3.957	253.3

[a] m is the number of spherical segments in the model; σ is the hard-core diameter; and ϵ and λ are the depth and range of the square-well dispersive interactions, respectively.

3.1. Linear Alkanes. Linear alkanes (*n*-alkanes) are the simplest homologous series of linear nonassociating molecules. The thermodynamic properties of *n*-alkanes have been studied extensively, with a particular emphasis on the fluid phase equilibria. In common with other SAFT studies, the *n*-alkanes are modeled as fully flexible chains formed from m united-atom segments (in this case, square-well segments); a more detailed atomic description of the structure can be used (e.g., see references 53−55), but such models are not considered here. The SAFT-VR equation of state has been used in a number of studies of the bulk fluid phase equilibria of pure *n*-alkanes and mixtures.[47,56−62] Here, we use the latest set of parameters[61,62] because this will provide a more accurate description of the vapor−liquid phase behavior of the longer *n*-alkanes (including the polymer limit, polyethylene) and is therefore expected to yield a reliable description of the vapor−liquid surface tension for these systems.

The vapor−liquid phase equilibria and surface tension for the first seven members of the *n*-alkane series (methane to *n*-heptane) are calculated with the SAFT-VR DFT approach for temperatures along the saturation line using the molecular parameters of reference;[61] for completeness, the parameters are given in Table 1. The vapor−liquid phase envelopes obtained with the SAFT-VR approach are shown in Figure 1a where they are compared with the experimental data.[63] The theory is seen to provide an excellent description of the vapor−liquid equilibria of the *n*-alkanes. Although not shown here, the vapor-pressure curves of the alkanes (and the other pure compounds studied in the current paper) are also very accurately described by the SAFT-VR approach. As expected for any classical equation of state, the SAFT-VR approach is seen to overestimate the experimental critical temperature in all cases.

The temperature dependence of the surface tension for *n*-alkanes obtained within the SAFT-VR DFT formalism is shown in Figure 1b. The agreement between the SAFT-VR DFT predictions and the experimental data is remarkable, considering that the parameters have not been refined to the experimental surface tension data. By contrast to the square-gradient approaches, no adjustable parameter is used to describe the interfacial data. According to our calculations, the values of the surface tension are overestimated in the neighborhood of the critical point due to the overestimate of the critical temperature. It is very gratifying to find that the predictions for the surface tension are in good agreement with experimental data, even for the longer alkanes. This is particularly encouraging, considering that the chain contribution is treated at the local level, an approximation which one may have anticipated to deteriorate for increasingly longer molecular chains. The ability of the theory to reproduce the relatively low values of the surface

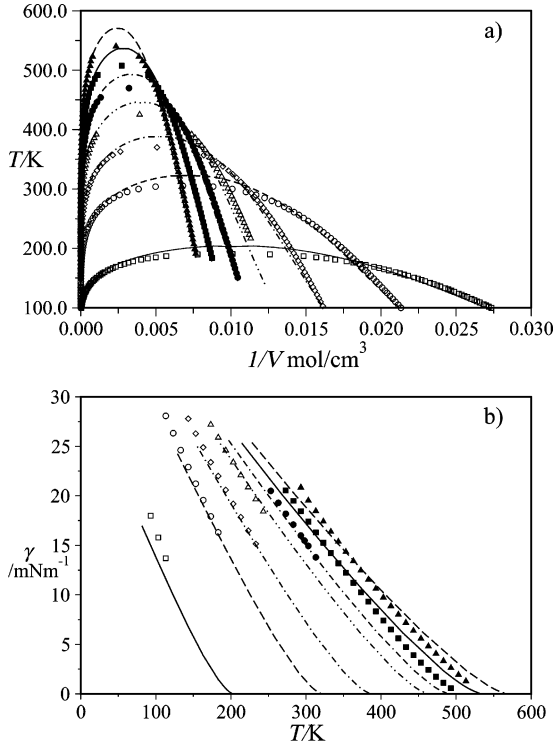

Figure 1. (a) Vapor−liquid coexistence densities, and (b) surface tension for the *n*-alkanes. The symbols represent the experimental data,[63] and the curves are the predictions of the SAFT-VR DFT approach with the parameters of Paricaud et al.[61] (see Table 1): methane (squares and continuous curves); ethane (circles and dashed curves); propane (diamonds and dotted−dashed curves); *n*-butane (triangles and double-dotted−dashed curves); *n*-pentane (filled circles and dotted-double−dashed curves); *n*-hexane (filled squares and continuous curves); and *n*-heptane (filled triangles and dashed curves).

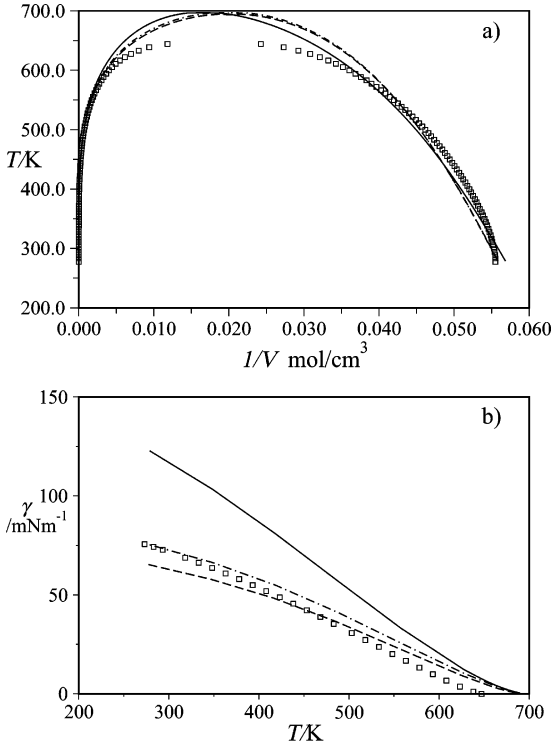

Figure 2. (a) Vapor−liquid coexistence densities, and (b) surface tension for water. The squares represent the experimental data,[63] and the curves are the values obtained with the SAFT-VR DFT approach using the parameters optimized to the vapor−liquid equilibria alone (VLE, continuous curves) and using the parameters optimized to the vapor−liquid equilibria and surface tension data (VLE + ST, set 1 correspond to the dashed curves, and set 2 to the dotted−dashed curves) given in Table 2.

tension of the *n*-alkanes can be regarded as a stringent test of the theoretical approach.

3.2. Small Associating Molecules. We now consider the interfacial properties of small associating molecules, focusing on water which is of fundamental importance and is particularly relevant in industrial applications.

Water is arguably the most widely studied associating system, but ironically, it is still one of the most difficult to model at a molecular level. Its properties are deeply conditioned by the extent of hydrogen bonding (every atom can participate in the association interaction). In common with other studies with Wertheim-like models (see ref 49 and references therein), we use a four-site model to represent the water molecule. Two of the sites are of type A (to account for the two hydrogen atoms of water), two are of type B (accouting for the oxygen lone pairs), and only A−B bonding is allowed. This allows for the formation of linear and branch chains and network-like structures in the fluid, as one would expect in water. The SAFT-VR molecular parameters obtained by regressing the vapor−liquid phase equilibria data[63] are presented in Table 2; these are very similar but not identical to the parameters used in the study of electrolyte solutions by Galindo et al.,[64] the difference being due to the different sets of experimental data used in the analysis.

The vapor−liquid envelope of water obtained by using the SAFT-VR equation of state is compared with experimental data[63] in Figure 2a. As expected, the molecular parameters are seen to provide a good description of the vapor−liquid phase envelope of water. The corresponding values of the surface tension obtained with this set of parameters using the SAFT-VR DFT approach are shown in Figure 2b as a function of temperature. Using this set of parameters, which are obtained from vapor−liquid equilibria alone, the theory predicts the correct sigmoidal shape of the surface tension curve (see reference 41 for an in-depth study of the nature of this behavior), but does not provide a quantitative agreement of the experimental data: the interfacial tension is overestimated with the SAFT-VR DFT method.

TABLE 2: SAFT-VR Square-Well Intermolecular Potential Parameters for Water Optimized to the Vapor−Liquid Equilibria Alone (VLE) and to the Vapor−Liquid Equilibria and Surface Tension Data (VLE + ST)[a]

substance	optimized to	m	λ	σ /Å	(ϵ/k) /K	(ϵ^{hb}/k) /K	r_c /σ
water	VLE	1.000	1.800	3.045	276.9	1315	0.676
water	VLE + ST(1)	1.000	1.800	3.011	174.3	1684	0.718
water	VLE + ST(2)	1.000	1.800	2.990	152.7	1771	0.725

[a] *m* is the number of spherical segments in the model; σ is the hard-core diameter; ϵ and λ are the depth and range of the square-well dispersive interactions, respectively; and ϵ^{hb} and r_c are the depth and range of the square-well associating sites, respectively.

As we mentioned previously, the vapor−liquid interfacial tension data can be used to obtain an "optimal" set of parameters for a given associating substance. The direct inclusion of the surface tension residuals in the objective function is difficult because of the computationally intensive nature of the solution of the Euler−Lagrange equation for the density profile with a DFT approach. The following intermediate "optimization" procedure is employed: the value of hydrogen-bonding energy ϵ^{hb} that best describes the surface tension of water at all temperatures is first determined using the original set of molecular parameters obtained from vapor−liquid experimental

data alone. Fixing ϵ^{hb} to this value, the remaining parameters (apart from the chain length parameter, which is kept as $m = 1$ for this near-spherical molecule) are then reoptimized to the bulk vapor−liquid equilibria data. Two "optimal" sets of parameters obtained with this procedure by considering both the vapor−liquid equilibria and surface tension data (VLE + ST) are collected in Table 2. The first set (1) provides the correct slope of the temperature dependence of the surface tension, and the second set (2), the best overall description of the surface tension data. As can be seen from Figure 2, the SAFT-VR DFT approach can be used to provide not only a good description of the vapor−liquid phase envelope but also a significantly improved description of the surface tension over the whole liquid range when the new sets of parameters are used. As for the *n*-alkanes, the main inadequacy of the theory is in the description of the critical region, which is even more problematic in the case of water. The use of the vapor−liquid interfacial tension data leads one to the conclusion that a larger hydrogen-bonding contribution (relative to the dispersion attractions) is required in modeling water than the one that results from an assessment of the bulk fluid phase equilibria. A similar conclusion was reached in the recent study of Wertheim models of water, in which the degree of association in water and the fluid phase equilibria of mixtures was used to develop "optimal" models of water.[49] Our current study is a clear example of the difficulty in decoupling the relative magnitude of the dispersive and associative attractive energies from an analysis of the vapor−liquid equilibria alone. Though numerical difficulties prevent us from employing an algorithm that includes the surface tension data in the objective function of a formal optimization scheme, our sequential approach is certainly a step in the right direction.

3.3. Linear Alkan-1-ols. Linear alkan-1-ols represent the simplest homologous series of molecules that include a chain-like structure and intermolecular association as the most important molecular features. These molecules are usually described as two-site (where one site accounts for the hydroxyl hydrogen, and the other the oxygen lone pairs taken together) or three-site (where one site represents the hydrogen atom and the other two the two oxygen lone pairs) models (e.g., see refs 41, 65−67). In the case of long-chain alkanols, however, steric effects can prevent all three sites from being involved in the bonding, and a two-site model can be preferable. Because the alkanols examined in this work were relatively short, we opt for a three-site description as it is more chemically intuitive; one should note, however, that the quality of the description of the fluid phase behavior and surface tension is comparable with the two- and three-site models. We employ the relationship between the chain length, *m* (molecular size asymmetry), and the number of carbon atoms, *C*, of the linear alcohol,

$$m = 1 + \frac{1}{3}(C - 1) + 0.2 \qquad (10)$$

developed in related SAFT-HS studies of the liquid−liquid equilibria of aqueous mixtures of alkyl polyoxyethylene ethers by García-Lisbona et al.;[68,69] linear alkan-1-ols can be considered as members of the series with no oxyethylene units. This allows us to fix the chain length during the optimization of parameters.

We thus start by refining the molecular parameters (segment size, dispersive energy, potential range, association energy, and bonding volume) of the three-site chain model by fitting to the experimental vapor pressure and saturated liquid density, from the triple point to the neighborhood (90%) of the critical point.[63] The sets of parameters refined to the experimental vapor−liquid envelope alone (see Table 3) provide an excellent description of the phase equilibria of linear 1-alcohols, but rather poor agreement with the experimental data for the surface tension (not shown). The parameter optimization scheme used for water is then used to obtain new sets of parameters for alkan-1-ols, which take into account the description of the interfacial tension (see Table 3). The predicted and experimental vapor−liquid phase envelopes of selected alkan-1-ols are shown in Figure 3a, where it is clear that SAFT-VR provides an excellent description in all cases over the whole liquid range. The temperature dependence of the surface tension is shown in Figure 3b. In all cases, the surface tension curves exhibit the inflected curvature characteristic of strongly hydrogen-bonded

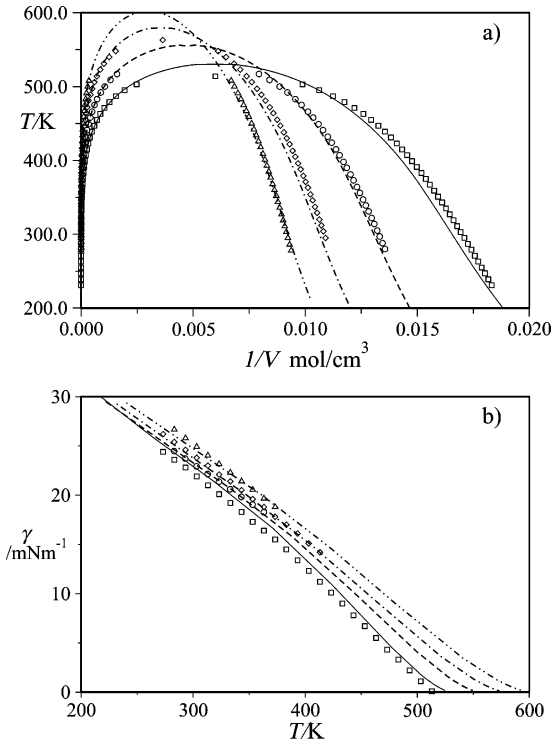

Figure 3. (a) Vapor−liquid coexistence densities, and (b) surface tension for the linear alkan-1-ols. The symbols represent the experimental data,[63] and the curves are the predictions of the SAFT-VR DFT approach with molecular parameters optimized to the vapor−liquid equilibria and surface tension data (VLE + ST): ethanol (squares and continuous curves), propan-1-ol (circles and dashed curves), butan-1-ol (diamonds and dotted−dashed curves), and pentan-1-ol (triangles and double-dotted−dashed curves). The parameter values are presented in Table 3.

TABLE 3: SAFT-VR Square-Well Intermolecular Potential Parameters for the Linear Alkan-1-ols Optimized to the Vapor−Liquid Equilibria Alone (VLE) and to the Vapor−Liquid Equilibria and Surface Tension Data (VLE + ST)[a]

substance	optimized to	m	λ	σ /Å	(ϵ/k) /K	(ϵ^{hb}/k) /K	r_c /σ
ethanol	VLE	1.533	1.800	3.699	183.5	1818	0.649
ethanol	VLE + ST	1.533	1.800	3.622	144.9	2940	0.607
propan-1-ol	VLE	1.866	1.697	3.758	216.8	2491	0.593
propan-1-ol	VLE + ST	1.866	1.720	3.605	166.4	2756	0.622
butan-1-ol	VLE	2.200	1.647	3.695	163.5	2992	0.663
butan-1-ol	VLE + ST	2.200	1.800	3.749	153.8	2823	0.623
pentan-1-ol	VLE	2.533	1.577	3.874	273.7	2296	0.599
pentan-1-ol	VLE + ST	2.533	1.800	3.761	157.9	2899	0.618

[a] *m* is the number of spherical segments in the model; σ is the hard-core diameter; ϵ and λ are the depth and range of the square-well dispersive interactions, respectively; and ϵ^{hb} and r_c are the depth and range of the square-well associating sites, respectively.

substances. We note that the values of the surface tension of linear alkan-1-ols exhibit a smaller variation along the series than was found for the *n*-alkanes. It is interesting to compare the values of the parameters obtained using both optimization procedures: using only the vapor−liquid data; and using the vapor−liquid and surface tension data together (see Table 3). There also appears to be a certain degree of transferability of the intermolecular parameters between different members of the alkan-1-ols series, which indicates that a successful group-contribution approach could be developed for the thermodynamic properties of these associating molecules.

3.4. Refrigerants. Refrigerants represent a class of chemical compounds of particular industrial importance. The first stable and nontoxic compounds used as refrigerants in the 1930s, the well-known chlorofluorocarbons (CFCs), have been replaced since 1987 due to the link between CFCs in the stratosphere and the depletion of the ozone layer. The most common alternative refrigerants are the hydrochlorofluorocarbons (HCFCs) and hydrofluorocarbons (HFCs). The presence of hydrogen atoms allows water-soluble compounds to be formed, which are removed from the atmosphere by rainfall. It is, therefore, particularly timely to have an accurate predictive platform for the thermodynamic properties of these systems, including the interfacial tension.

Here, we consider four representative replacement refrigerants: difluoromethane (HFC-32), chlorodifluoromethane (HCFC-22), 1,1,1,2-tetrafluoroethane (HFC-134a), and pentafluoroethane (HFC-135). These molecules are characterized by anisotropies in the molecular shape, the presence of permanent (or induced) polar interactions, or both. Following Galindo et al.,[70] we model these molecules as chains of m spherical segments interacting through square-well intermolecular potentials of variable range, with a number of embedded off-center, square-well bonding sites. The short-ranged attractive sites mediate molecular association, and they can also be used to represent the physical features, in a geometrical sense, of short-range anisotropic polar interactions. In the case of the HFC-32 refrigerant four sites (two of type A and two of type B, with only A−B bonding) are included on a central spherical core ($m = 1$) to account for the anisotropy of the electrostatic interactions. The HFC-22, HFC-134a, and HFC-125 refrigerants are modeled with two sites (one of type A and one of type B, with only A−B bonding); HFC-22 is treated as a spherical molecule ($m = 1$), and HFC-134a and HFC-125 are nonspherical ($m > 1$). It is important to note that experimental neutron-scattering data for a similar system, trifluoromethane (HFC-24), suggest that these molecules do not form hydrogen bonds.[71] Though our models for these refrigerants do not include an explicit contribution from the polar interactions, the bonding sites are incorporated in the hope that this will capture aspects of the polar anisotropy. The molecular parameters for the refrigerants studied by Galindo et al.[70] are given in Table 4; also included are the parameters obtained here for HFC-22.

The vapor−liquid phase envelope for HFC-32 is depicted in Figure 4a. Agreement between the theoretical predictions (with the parameters of Galindo et al.[70]) and experimental data[63] is excellent over the whole liquid range. The temperature dependence of the surface tension is presented in Figure 4b. As was shown in previous work,[38,41] the curvature of $\gamma(T)$ is very sensitive to the nature of the association. For nonassociating systems, such as the *n*-alkanes, the curvature of $\gamma(T)$ is always positive. For associating systems with anisotropic interactions, $\gamma(T)$ exhibits a point of inflection at intermediate temperatures, where the curvature changes sign and a characteristic s-shape

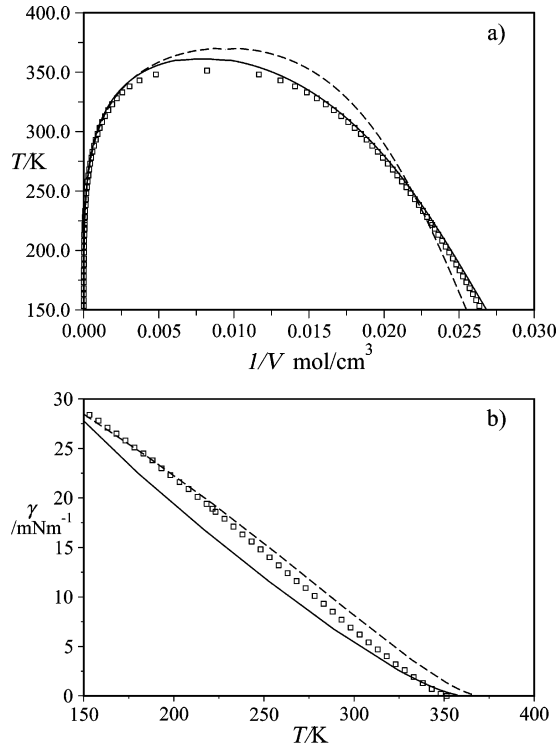

Figure 4. (a) Vapor−liquid coexistence densities, and (b) surface tension for the refrigerant difluoromethane (HFC-32). The squares represent the experimental data,[63] and the curves are the values obtained with the SAFT-VR DFT approach using the parameters optimized to the vapor−liquid equilibria alone (VLE, continuous curves) and using the parameters optimized to the vapor−liquid equilibria and surface tension data (VLE + ST, dashed curves) reported in Table 4.

TABLE 4: SAFT-VR Square-Well Intermolecular Potential Parameters for Selected Replacement Refrigerants Optimized to the Vapor−Liquid Equilibria Alone (VLE) and to the Vapor−Liquid Equilibria and Surface Tension Data (VLE + ST)[a]

substance	optimized to	m	λ	σ /Å	(ϵ/k) /K	(ϵ^{hb}/k) /K	r_c /σ
HFC-32	VLE	1.000	1.239	4.116	259.3	619.3	0.808
HFC-32	VLE+ST	1.000	1.350	4.070	234.3	684.3	0.747
HFC-22	VLE	1.000	1.790	4.553	175.6	1038	0.634
HFC-22	VLE+ST	1.000	1.287	4.900	415.2	375.8	0.671
HFC-134a	VLE	1.400	1.850	3.974	122.7	1301	0.715
HFC-134a	VLE+ST	1.400	1.900	4.041	127.7	1197	0.761
HFC-125	VLE	1.350	1.360	4.535	303.8	724.8	0.669
HFC-125	VLE+ST	1.350	1.257	4.630	323.7	446.8	0.990

[a] m is the number of spherical segments in the model; σ is the hard-core diameter; ϵ and λ are the depth and range of the square-well dispersive interactions, respectively; and ϵ^{hb} and r_c are the depth and range of the square-well associating sites, respectively.

behavior is seen. This is, indeed, the case of HFC-32. Once again, our theoretical approach fails to reproduce the experimental surface tension data when implemented with parameters obtained from experimental vapor−liquid data alone: in contrast to the experimental behavior, the $\gamma(T)$ curve is predicted to be concave-up throughout the whole of the liquid range. By following the procedure described for water, we then determine a new set of parameters by including the experimental surface tension data in the refinement. The resulting values of the molecular parameters, also included in Table 4, provide a better description of the shape of the surface tension curve. It is interesting to note that the parameters of Galindo et al.[70] are consistent with a range of association (bonding volume) that is

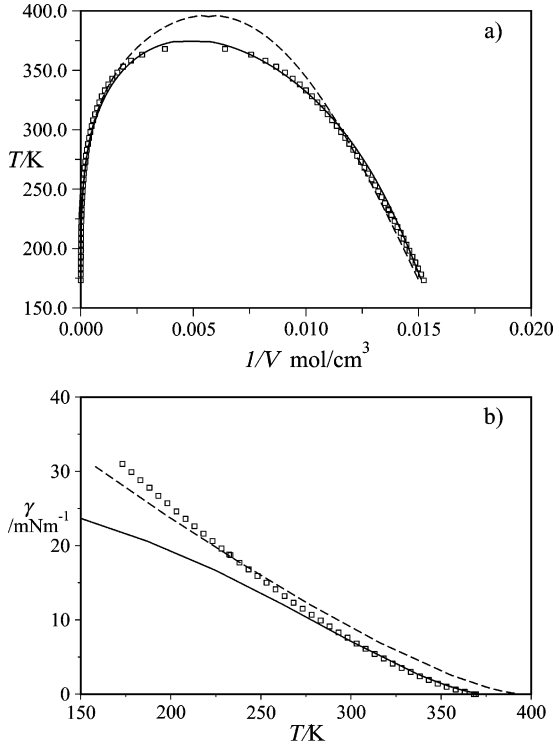

Figure 5. (a) Vapor−liquid coexistence densities, and (b) surface tension for the refrigerant chlorodifluoromethane (HCFC-22). The squares represent the experimental data,[63] and the curves are the values obtained with the SAFT-VR DFT approach using the parameters optimized to the vapor−liquid equilibria alone (VLE, continuous curves) and using the parameters optimized to the vapor−liquid equilibria and surface tension data (VLE + ST, dashed curves) reported in Table 4.

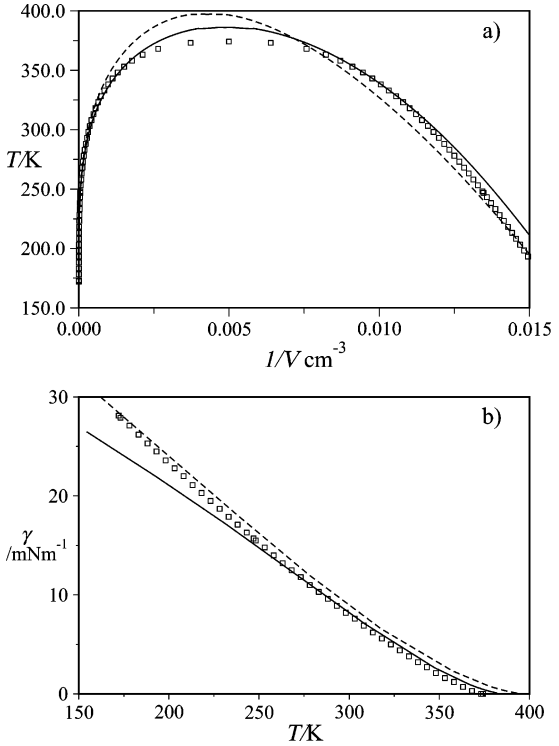

Figure 6. (a) Vapor−liquid coexistence densities, and (b) surface tension for the refrigerant 1,1,1,2-tetrafluoroethane (HFC-134a). The squares represent the experimental data,[63] and the curves are the values obtained with the SAFT-VR DFT approach using the parameters optimized to the vapor−liquid equilibria alone (VLE, continuous curves) and using the parameters optimized to the vapor−liquid equilibria and surface tension data (VLE + ST, dashed curves) reported in Table 4.

larger than that obtained here, whereas the range of the dispersive interaction is shorter.

The refrigerant HFC-22 is modeled in a similar way with a single square-well core and two off-center bonding sites. Molecular parameters obtained by fitting to the experimental vapor−liquid phase equilibria alone and to the phase equilibria and surface tension data are given in Table 4. In Figure 5, we show a comparison between the experimental vapor−liquid phase envelope and surface tension, and the corresponding theoretical predictions. The theory with the new values of the molecular parameters provides the correct curvature for the temperature dependence of the surface tension while still accurately capturing the vapor−liquid phase envelope.

We now consider the phase equilibria and surface tension of HFC-134a. Contrary to the case of HFC-32 and HFC-22, which are modeled as spherical molecules, HFC-134a is described as two fused, hard-spherical segments characterized by a value of $m = 1.4$, which accounts for the asymmetry in the molecular shape; m must now be incorporated into the optimization scheme. The HFC-134a parameter values obtained by Galindo et al.[70] are also included in Table 4. The SAFT-VR equation of state provides a good description of the vapor−liquid phase envelope (see Figure 6a) with these parameters, but again the SAFT-VR DFT approach does not provide the correct shape of the surface tension curve over the whole liquid range (see Figure 6b); the largest deviations can be seen at low temperatures. As for HFC-32 and HFC-22, a better description of the surface tension can be obtained by including this data in the refinement of the parameters. The representation of the fluid phase equilibria is not as good with the new set of molecular parameters, as may have been anticipated.

Finally, we consider HFC-125, which is modeled in a way similar to HFC-134a. The sets of parameters refined to vapor−liquid equilibria alone (VLE)[70] and to the vapor−liquid equilibria and surface tension (VLE + ST) are reported in Table 4. As shown in Figure 7, SAFT-VR provides an excellent description of both the phase envelope and the surface tension for both sets of parameters. Only a marginal improvement in the representation of the surface tension is achieved in this case by including the data in the fit.

Conclusion

We use a recently proposed density functional theory with the SAFT-VR approach to predict the vapor−liquid interfacial properties of representative examples of nonassociating and associating chain molecules. The free energy functional is divided into a reference term (which accounts for the ideal, hard-sphere, chain, and association contributions) and a perturbative term (which includes the dispersive attractive interactions between the monomeric segments). The effect of short ranged correlations between the segments are accounted for in the reference term, which is treated with a local density approximation. The long-range segment−segment correlations are included in the attractive perturbation term by using an average correlation function of a reference hard-sphere fluid.

The surface tension of selected linear alkanes is examined first. The molecular parameters obtained from a fit to the vapor−liquid equilibria are used to predict the surface tension of different members of the *n*-alkane series. The theory is seen to provide an excellent description of this property for these nonpolar molecules. The theoretical description of the phase equilibria and interfacial properties of selected associating substances (water, linear alkan-1-ols, and HFCs) with several

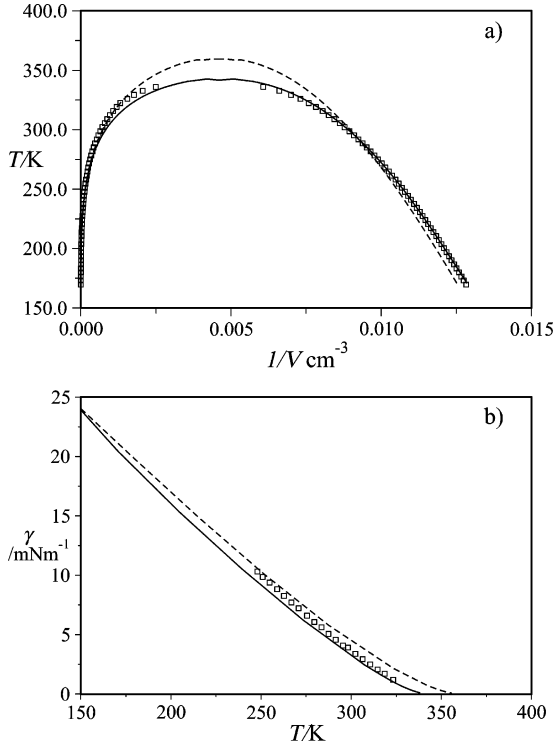

Figure 7. (a) Vapor−liquid coexistence densities, and (b) surface tension for the refrigerant pentafluoroethane (HFC-125). The squares represent the experimental data,[63] and the curves are the values obtained with the SAFT-VR DFT approach using the parameters optimized to the vapor−liquid equilibria alone (VLE, continuous curves) and using the parameters optimized to the vapor−liquid equilibria and surface tension data (VLE + ST, dashed curves) reported in Table 4.

association schemes is then undertaken. For molecular parameters refined to the fluid phase equilibria alone, the description of the surface tension with the SAFT-VR DFT approach is generally inadequate. A good description of both the vapor−liquid equilibria and surface tension can be achieved by including interfacial data in the optimization scheme. This type of procedure for the estimation of intermolecular parameters is rare; the only other work that we are aware of is that of Neimark et al.,[72] who have used the bulk phase behavior and interfacial tension to develop models of argon and nitrogen in a nonlocal DFT study of the adsorption of the gases in nanoporous materials.

Our approach can help to solve the problem of estimating SAFT parameters for associating compounds where a number of different sets of parameters can describe the experimental vapor−liquid equilibria in an apparently equivalent manner (cf. reference 49). The degeneracy of the molecular parameters for associating substances is due in part to the strong dependence of the vapor−liquid equilibria on the total cohesive (dispersive and associative) energy and not to the precise partitioning of the various contributions. The use of additional properties, such as the interfacial tension, the extent of association, and the fluid phase equilibria of mixtures, allows one to obtain more reliable molecular parameters, which can be used with confidence over a range of conditions.

Acknowledgment. G.J.G. thanks BP Exploration for funding a studentship. We acknowledge further support from the Engineering and Physical Sciences Research Council (EPSRC) (Grants GR/N20317, GR/N03358, GR/N35991, GR/R09497, and EP/E016340), the Joint Research Equipment Initiative (JREI) for computer hardware (GR/M94427), and the Royal Society-Wolfson Foundation for the award of a refurbishment grant. F.J.B., E.M.dR. and E.dM. are also grateful for financial support from project number FIS2004-06227-C02-01 of the Spanish DGICYT (Dirección General de Investigación Científica y Técnica), as well as for additional financial support from the Universidad de Huelva and the Junta de Andalucía.

References and Notes

(1) van der Waals, J. D. *Z. Phys. Chem.* **1894**, *13*, 657; translation by Rowlinson, J. S. *J. Stat. Phys.* **1979**, *20*, 197.
(2) Rowlinson, J. S.; Widom, B. *Molecular Theory of Capillarity*; Clarendon Press: Oxford, 1982.
(3) *Fundamentals of Inhomogeneous Fluids*; Henderson, D, Ed.; Dekker: New York, 1992.
(4) *Equations of State for Fluids and Fluid Mixtures*, Parts 1 and 2; Senger, J. V., Kayser, K. E., Peter, C. J., White, H. J., Jr., Eds.; Elsevier: Amsterdam, 2000.
(5) Chapman, W. G.; Gubbins, K. E.; Jackson, G.; Radosz, M. *Fluid Phase Equilib.* **1989**, *52*, 31.
(6) Chapman, W. G.; Gubbins, K. E.; Jackson, G.; Radosz, M. *Ind. Eng. Chem. Res.* **1990**, *29*, 1709.
(7) Wertheim, M. S. *J. Stat. Phys.* **1984**, *35*, 19.
(8) Wertheim, M. S. *J. Stat. Phys.* **1984**, *35*, 35.
(9) Wertheim, M. S. *J. Stat. Phys.* **1986**, *42*, 459.
(10) Wertheim, M. S. *J. Stat. Phys.* **1986**, *42*, 477.
(11) Jackson, G.; Chapman, W. G.; Gubbins, K. E. *Mol. Phys.* **1988**, *65*, 1.
(12) Chapman, W. G.; Jackson, G.; Gubbins, K. E. *Mol. Phys.* **1988**, *65*, 1057.
(13) Galindo, A.; Burton, S. J.; Jackson, G.; Visco, D. P.; Kofke, D. *Mol. Phys.* **2002**, *100*, 2241.
(14) Hansen, J.-P.; McDonald, I. R. *Theory of Simple Liquids*, 3rd ed.; Academic Press: New York, 2006.
(15) Müller, E. A.; Gubbins, K. E. A review of SAFT and related approaches. In *Equations of State for Fluids and Fluid Mixtures*, Part 2; Sengers, J. V., Kayser, R. F., Peters, C. J., White, H. J., Jr., Eds.; Elsevier: Amsterdam, 2000.
(16) Müller, E. A.; Gubbins, K. E. *Ind. Eng. Chem. Res.* **2001**, *40*, 2193.
(17) Evans, R. Density Functionals in the Theory of Nonuniform Fluids. In *Fundamentals of Inhomogeneous Fluids*; Henderson, D., Ed.; Dekker: New York, 1992.
(18) Macleod, D. B. *Trans. Faraday Soc.* **1923**, *19*, 38.
(19) Weinaug, C. F.; Katz, D. L. *Ind. Eng. Chem.* **1943**, *35*, 239.
(20) Fowler, R. H. *Proc. R. Soc., Ser. A* **1937**, *159*, 229.
(21) Guggenheim, E. A. *J. Chem. Phys.* **1945**, *13*, 253.
(22) Zuo, Y.-X.; Stenby, E. H. *Can. J. Chem. Eng.* **1997**, *75*, 1130.
(23) Cahn, J. W.; Hilliard, J. E. *J. Chem. Phys.* **1958**, *28*, 258.
(24) Carey, B. S.; Scriven, L. E.; Davies, H. T. *AIChE J.* **1980**, *26*, 705.
(25) Abbas, S.; Nordholm, S. *J. Colloid Interface Sci.* **1994**, *166*, 481.
(26) Cornelisse, P. M. W.; Peters, C. J.; de Swaan Arons, J. *J. Chem. Phys.* **1997**, *106*, 9820.
(27) Kahl, H.; Enders, S. *Fluid Phase Equiib.* **2000**, *172*, 27.
(28) Kahl, H.; Enders, S. *Phys. Chem. Chem. Phys.* **2002**, *4*, 931.
(29) Pàmies, J. C. Ph.D. Thesis, Universitat Rovira i Virgili, 2003.
(30) Duque, D.; Pàmies, J. C.; Vega, L. F. *J. Chem. Phys.* **2004**, *121*, 11395.
(31) McCabe, C.; Kiselev, S. B. *Ind. Eng. Chem. Res.* **2004**, *43*, 2839.
(32) Mejía, A.; Pàmies, J. C.; Duque, D.; Segura, H.; Vega, L. F. *J. Chem. Phys.* **2005**, *123*, 034505.
(33) Mejía, A.; Segura, H.; Wisniak, J.; Polishuk, I. *Phys. Chem. Liq.* **2006**, *44*, 45.
(34) Fu, D.; Li, X.-S.; Yan, S.; Liao, T. *Ind. Eng. Chem. Res.* **2006**, *45*, 8199.
(35) Davis, H. T. *Statistical Mechanics of Phases and Interfaces, and Thin Films*; VCH: Weinheim, 1996.
(36) Winkelmann, J. *J. Phys.: Condens. Matter* **2001**, *13*, 4739.
(37) Wu, J. *AIChE J.* **2006**, *52*, 1169.
(38) Blas, F. J.; Martín del Río, E.; de Miguel, E.; Jackson, G. *Mol. Phys.* **2001**, *99*, 1851.
(39) Gloor, G. J.; Blas, F. J.; Martín del Río, E.; de Miguel, E.; Jackson, G. *Fluid Phase Equilib.* **2002**, 521, 194−197.
(40) Gloor, G. J. Ph.D. Thesis, Imperial College London, 2003.
(41) Gloor, G. J.; Jackson, G.; Blas, F. J.; Martín del Río, E.; de Miguel, E. *J. Chem. Phys.* **2004**, *121*, 12740.
(42) Fu, D.; Zhao, Y. *Chin. J. Chem.* **2005**, *23*, 386.
(43) Fu, D.; Wu, J. *Ind. Eng. Chem. Res.* **2005**, *44*, 1120.
(44) Tripathi, S.; Chapman, W. G. *Phys. Rev. Lett.* **2005**, *94*, 087801.
(45) Tripathi, S.; Chapman, W. G. *J. Chem. Phys.* **2005**, *122*, 094506.
(46) Dominik, A.; Tripathi, S.; Chapman, W. G. *Ind. Eng. Chem. Res.* **2006**, *45*, 6785.

(47) Gil-Villegas, A.; Galindo, A.; Whitehead, P. J.; Mills, S. J.; Jackson, G.; Burgess, A. N. *J. Chem. Phys.* **1997**, *106*, 4168.
(48) Toxvaerd, S. *J. Chem. Phys.* **1976**, *64*, 2863.
(49) Clark, G. N. I.; Haslam, A. J.; Galindo, A.; Jackson, G. *Mol. Phys.* **2006**, *104*, 3561.
(50) Carnahan, N. F.; Starling, K. E. *J. Chem. Phys.* **1969**, *51*, 635.
(51) Barker, J. A.; Henderson, D. *Rev. Mod. Phys.* **1976**, *48*, 587.
(52) Press, W. H.; Flannery, B. P.; Teukolsky, S. A.; Vetterling, W. T. *Numerical Recipes in FORTRAN: The Art of Scientific Computing*, 2nd ed. Cambridge University Press: New York, 1992.
(53) Sear, R. P.; Amos, M. D.; Jackson, G. *Mol. Phys.* **1993**, *80*, 777.
(54) Archer, A. L.; Amos, M. D.; Jackson, G.; McLure, I. A. *Int. J. Thermophys.* **1996**, *17*, 201.
(55) McCabe, C.; Gil-Villegas, A.; Jackson, G.; del Río, F. *Mol. Phys.* **1999**, *97*, 551.
(56) McCabe, C.; Gil-Villegas, A.; Jackson, G. *J. Phys. Chem. B* **1998**, *102*, 4183.
(57) McCabe, C.; Galindo, A.; Gil-Villegas, A.; Jackson, G. *J. Phys. Chem. B.* **1998**, *102*, 8060.
(58) McCabe, C.; Galindo, A.; Gil-Villegas, A.; Jackson, G. *Int. J. Thermophys.* **1998**, *19*, 1511.
(59) McCabe, C.; Jackson, G. *Phys. Chem. Chem. Phys.* **1999**, *1*, 2057.
(60) McCabe, C.; Galindo, A.; García-Lisbona, M. N.; Jackson, G. *Ind. Eng. Chem. Res.* **2001**, *40*, 3835.
(61) Paricaud, P.; Galindo, A.; Jackson, G. *Ind. Eng. Chem. Res.* **2004**, *43*, 6871.
(62) Haslam, A. J.; von Solms, N.; Adjiman, C. S.; Galindo, A.; Jackson, G.; Paricaud, P.; Michelsen, M. L.; Kontogeorgios, G. M. *Fluid Phase Equilib.* **2006**, *243*, 74.
(63) Fletcher, D. A.; McMeeking, R. F.; Parkin, D. *J. Chem. Inf. Comput. Sci.* **1996**, *36*, 746.
(64) Galindo, A.; Gil-Villegas, A.; Jackson, G.; Burgess, A. N. *J. Phys. Chem. B* **1999**, *103*, 10272.
(65) Nezbeda, I.; Kolafa, J.; Smith, W. R. *Fluid Phase Equilib.* **1997**, *130*, 133.
(66) Smith, W. R.; Nezbeda, I. *J. Chem. Phys.* **1984**, *81*, 3694.
(67) Nezbeda, I.; Pavlicek, J.; Kolafa, J.; Galindo, A.; Jackson, G. *Fluid Phase Equilib.* **1999**, *193*, 158−160.
(68) García-Lisbona, M. N.; Galindo, A.; Jackson, G.; Burgess, A. N. *Mol. Phys.* **1998**, *93*, 57.
(69) García-Lisbona, M. N.; Galindo, A.; Jackson, G.; Burgess, A. N. *J. Am. Chem. Soc.* **1998**, *120*, 4191.
(70) Galindo, A.; Gil-Villegas, A.; Whitehead, P. J.; Jackson, G.; Burgess, A. N. *J. Phys. Chem. B* **1998**, *102*, 7632.
(71) Mort, K. A.; Johnson, K. A.; Cooper, D. L.; Burgess, A. N.; Howells, W. S. *Mol. Phys.* **1997**, *90*, 415.
(72) Neimark, A. V.; Ravikovitch, P. I.; Grün, M.; Schüth, F.; Unger, K. K. *J. Colloid Interface Sci.* **1998**, *207*, 159.